

Reactive Lattice Gas Model for FitzHugh-Nagumo Dynamics

Anatoly Malevanets and Raymond Kapral
Chemical Physics Theory Group, Department of Chemistry,
University of Toronto, Toronto, Ontario M5S 3H6, Canada

September 4, 1997

The FitzHugh-Nagumo reaction-diffusion equation [1]

$$\begin{aligned}u_\tau &= -u^3 + u - v + D_u \nabla^2 u, \\v_\tau &= \epsilon(u - \alpha v - \beta) + D_v \nabla^2 v,\end{aligned}\tag{1}$$

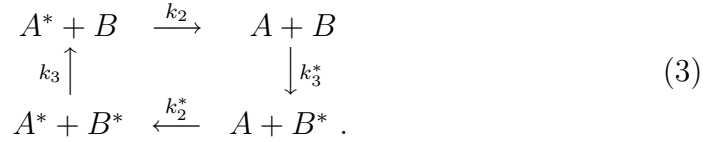
and models with a similar structure of S-shaped and linear nullclines for the reaction terms, have been used to investigate a variety of unusual front bifurcation and pattern formation processes. [2, 3, 4] Such studies have provided interpretations of the origin of labyrinthine and complex spiral wave patterns seen in experiments on the iodide-ferrocyanide-sulfite system [5].

It is interesting to examine such complex pattern-forming systems from a microscopic point of view that incorporates both molecular fluctuations and the correlations that exist between the reaction and diffusion processes. [6] In this way one may understand how macroscopic pattern formation arises from dynamics on the microscales and determine the conditions under which the macroscopic description based on the reaction-diffusion equation will break down. Phenomena such as phase transitions, which depend on the existence of fluctuations, may be studied and, in general, one may construct a nonequilibrium statistical mechanics for these systems.

For these reasons we have sought to find a microscopic chemical reaction dynamics whose mass action law is the FitzHugh-Nagumo equation. Based on this reaction kinetics, one may then construct a Markov chain model for both reaction and diffusion to describe the dynamics of the spatially-distributed reacting system. Below we show how the Markov chain dynamics

may be implemented as a lattice gas cellular automaton model and, as an illustration, present results for two-dimensional simulations of labyrinthine and Bloch front patterns, and three-dimensional simulations of links, knots and labyrinthine structures. [7, 8]

The model involves a two-species, site-specific reaction scheme on a cubic lattice where sites can accommodate up to N particles. Consider the following reaction scheme:



We suppose that each local site can accommodate a maximum of N particles of species A and B . The vacancies corresponding to these species will be denoted by A^* and B^* , respectively. Let a and b denote the concentrations per site of A and B . Then $a^* = 1 - a$ and $b^* = 1 - b$. With this local conservation law we may now write the mass-action rate law corresponding to the mechanism in (2) and (3) as

$$a_t = [k_1 a - k_1^*(1 - a)]a(1 - a) + k_2(1 - a)b - k_2^*a(1 - b) \quad (4)$$

$$b_t = k_3(1 - a)(1 - b) - k_3^*ab \quad (5)$$

If we take $k_2 = k_2^*$ and $k_3 = k_3^*$, introduce the change of variables $a = c_a u + a_0$ and $b = c_b v + b_0$, where the constants are defined by

$$\begin{aligned} c_a^2 &= \frac{1}{3} \left(\frac{k_1 + 2k_1^*}{k_1 + k_1^*} \right)^2 - \frac{k_2 + k_1^*}{k_1 + k_1^*}, \quad a_0 = \frac{1}{3} \frac{k_1 + 2k_1^*}{k_1 + k_1^*}, \\ c_b &= -\frac{k_1 + k_1^*}{k_2} c_a^3, \quad b_0 = a_0 \frac{c_b}{c_a} \left\{ 1 - \left(\frac{a_0}{c_a} \right)^2 \right\}, \end{aligned} \quad (6)$$

and scale the time as $\tau = t/\tau$ with $\tau_s^{-1} = (k_1 + k_1^*)c_a^2$, we recover the reactive terms in the FitzHugh-Nagumo equation (1). The reaction parameters in (1) are related to those in the mechanism by

$$\alpha = -\frac{c_b}{c_a}, \quad \beta = \frac{1 - a_0 - b_0}{c_a}, \quad \epsilon = \frac{k_3}{k_2} \left(\frac{c_a}{c_b} \right)^2. \quad (7)$$

This allows us to simulate the FitzHugh-Nagumo model for any desired values of the parameters simply by tuning the rate constants in the mechanism.

In the microscopic model the above reactions are described probabilistically by birth-death rules in the following way. The probability of occurrence of a particular reaction is proportional to the number of possible combinations of particles participating in a reaction step and the reaction rate constant of that step. The set of reactions (2) and (3) provides a specification how reactions takes place when particles collide in a local spatial volume. Spatio-temporal structures arise from the interplay between the local reactive collision dynamics and subsequent transfer of information through the medium that occurs as a result of the random walks that the particles make on the lattice.

The random walk dynamics is realized by use of an auxiliary “excited” particle lattice. At each step at most one particle per site is transferred to the excited state with a probability depending on the site occupation number. Next, the excited particles are translated one lattice unit in a random direction chosen from a set $V = \{\mathbf{v}_1, \dots, \mathbf{v}_k\}$. Finally, the excited particles are placed in new lattice positions. For the three-dimensional simulations, rather than using the simple cubic lattice, we have taken the set V to represent the projections of the normals of the four-dimensional FCC Wigner-Seitz cell on the three-dimensional space[9]. The fact that only a maximum of N particles of each species may reside at a node (exclusion principle) requires a vacancy to exist at a site in order to be able to accommodate a particle from the excited sublattice. In addition, we cannot create an excited particle from the vacuum, so that we have two restrictions on the excitation probability: $p(N) = 1$ and $p(0) = 1$. We found that the choice of a linear dependence of the excitation probability on the site occupation number leads to a concentration-independent diffusion coefficient. The diffusion rule leads to mixing of particles on the lattice and, to a good approximation, it establishes a local binomial probability distribution of particle numbers[8]. The use of a 24-direction diffusion rule is motivated by symmetry considerations. The FCC set of directions given by the six permutations of $(\pm 1, \pm 1, 0, 0)$ leads to a spherically symmetric discrete Laplacian with fourth-order corrections in the lattice spacing.

Reaction dynamics at a site is governed by a pair of random numbers (ν, ξ) where $\nu = \{1, \dots, 6\}$ and $\xi \in [0, 1]$. During a reaction step, one of the six reactions is chosen according to the random variable ν and is carried out if the number of possible choices of particles and vacancies participating in

the reaction times the reaction rate constant k_ν is greater than the random number ξ . Consider as an example the reaction channel



The number of ways to choose an ordered pair of particles and a vacancy is $n(n-1)(N-n)$ where n is the number of A particles at the site. If comparison is performed with a continuous, uniformly-distributed, random variable ξ , the probability of carrying out the reaction, creation of a particle in this case, is

$$P(2A + A^* \longrightarrow 3A) = P(\bar{k}_1 n(n-1)(N-n) > \xi). \quad (9)$$

Here $\bar{k}_1 = k_1/(N(N-1))$. The factor $N(N-1)$ is included so that the mass action law has standard form (cf. below). An important feature of the above rule, and the microscopic dynamics in general, is the fact that the exclusion principle is automatically satisfied due to the conversion between particles and vacancies during reactive collisions. In the limit that the site distribution is binomial and characterized by the mean particle density, the reaction rate for each channel, computed from the average of the particle number change times the channel reaction probability over the binomial distribution, is just that corresponding to mass action kinetics. For the example given above we have:

$$R_1(a) = \sum_n \bar{k}_1 n(n-1)(N-n) p_A^B(n; a) = k_1 a^2 (1-a) , \quad (10)$$

where $p_A^B(n; a) = \binom{N}{n} a^n (1-a)^{N-n}$ is the binomial distribution with a the average density of species A . A similar calculation may be carried out for each of the six reaction channels. After rescaling, the one obtains the FitzHugh-Nagumo mass action rate law. [8]

One may also show that when diffusion dominates reaction the local collision rules, together with the collective particle random walk dynamics, yields the FitzHugh-Nagumo reaction-diffusion equation (1) for the evolution of the local average particle densities. [8] Thus, one has a microscopic scheme whose macroscopic limit corresponds to the phenomenological reaction-diffusion equation description of FitzHugh-Nagumo kinetics.

Next, we describe the results of two and three-dimensional simulations to illustrate that the model can be used to study the dynamics in the reaction-diffusion regime where rather complex bistable structures exist as a result of

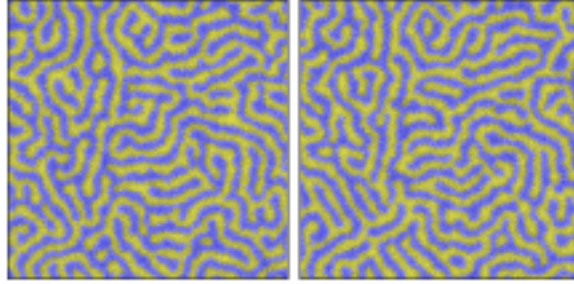


Figure 1: Snapshots of time evolution of a two-dimensional labyrinthine pattern. Reaction rate constants are $\bar{k}_1 = 3.84$, $\bar{k}_2 = 0.3$, $\bar{k}_3 = 0.2$ and $D_u/D_v = 4$.

competition between the curvature effects and front repulsion. The simulations were carried out on the CAM-8 machine. [10] First, consider pattern formation in two spatial dimensions. We may distinguish two regimes of front dynamics: the Ising and Bloch regimes. [11, 3] In the Ising regime a single front solution consists of the two stable states. When the diffusion ratio D_v/D_u is small enough evolution from the unstable state shows domain coarsening, similar to Model A of critical phenomena. [12] For larger values of D_v/D_u front repulsion is possible and when D_v/D_u is sufficiently large planar fronts may become unstable and a labyrinthine pattern is formed. Figure 1 shows the effect of fluctuations on such a labyrinthine pattern. In contrast the deterministic case where a stationary labyrinthine pattern formed, here fluctuations lead to rupture and fusion of labyrinthine bands and a time dependent pattern.

In the Bloch regime the front velocity has undergone a pitchfork bifurcation. the resulting Bloch fronts have two different velocities. As a result, even for symmetric bistable states, it is possible to form fronts where each phase consumes the other (cf. Fig. 2).

A new class of chemical patterns is possible in three spatial dimensions: stable, compact linked and knotted structures. We discuss the conditions under which these objects may be created and their stability. The aforementioned, three-dimensional structures are built on two-dimensional stable objects with radially symmetric concentration profiles. These two-dimensional patterns were analyzed in [2] and we note that such localized patterns were observed in chemical experiments. [13]

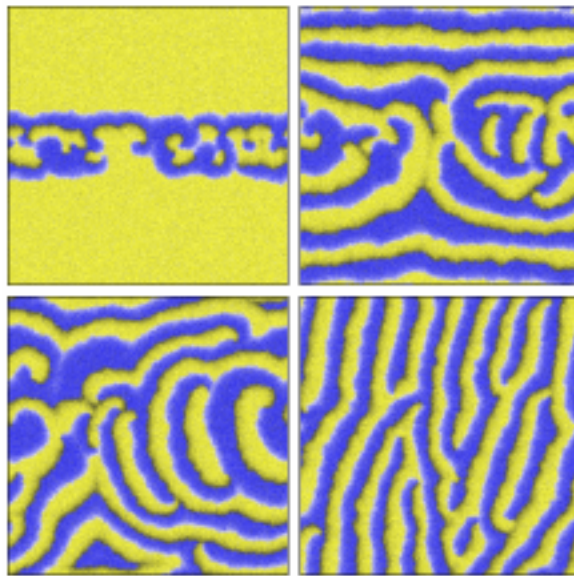


Figure 2: Evolution of Bloch fronts. Reaction rate constants are $\bar{k}_1 = 3.84$, $\bar{k}_2 = 0.23$, $\bar{k}_3 = 0.06$ and $D_u = 0$. Panels (top to bottom and left to right) correspond to 5, 20, 50, 300 ($\times 1,000$) automation steps.

We now present the results of simulations on three-dimensional tubular structures whose cross-sections are two-dimensional stable spots. In the simplest case an extension of a stable spot to a three-dimensional periodic domain is a stable straight tube. As for a stripe in two-dimensions, the tube may undergo a three dimensional transverse instability, leading to the analog of a labyrinthine instability. One may distinguish two distinct possibilities for the development of such instability. One, which we call a “branching instability”, is characterized by sprouting of new branches, stemming perpendicular to an existing segment. This instability strongly resembles the two-dimensional labyrinthine instability. In a confined domain the instability leads to the creation of a tree-like structure filling the domain as shown in Fig. 3. The second possibility is an increase in the length of the tubular domain without significant changes in the cross-section of the concentration profile. Its analog has not been reported in two-dimensional systems with FHN dynamics. The evolution of the system in this second regime fills the volume with a convoluted tube.

The existence of stable compact structures built from such tubes is an interesting phenomenon. Some examples were reported in [7]. Here we further discuss the conditions for the existence of such objects. For a system with parameter values ensuring the stability of a straight tube, one may attempt to connect the loose ends of a linear segment of the tubular domain and produce a stable solid torus pattern. We did not succeed in creating a viable torus by this approach. However two such tori connected in a Hopf link proved to be a stable object. In this case mutual repulsion between the tori balances the contraction driven by curvature. This is the simplest non-trivial compact stable structure observed in the simulations. (see Fig. 4) The stability of a Hopf link is not guaranteed by just existence of a stable spot and a tendency of a tubular domain to contract. There is necessarily an additional requirement for a sufficient repulsion between fronts. For an example in simulations shown in Fig. 5 a collision between the two tori led to the rupture of one of them and subsequent contraction of the objects to spheres.

It is also possible to form objects with knotted topologies if the initial tubular domain is knotted. Figure 6 shows a stable trefoil. Stable figure-8 knots have also been constructed [7] but larger volumes are needed for more complex knots.

Using the microscopic model described here one may investigate a number of fundamental questions concerning the origin of pattern formations in far-

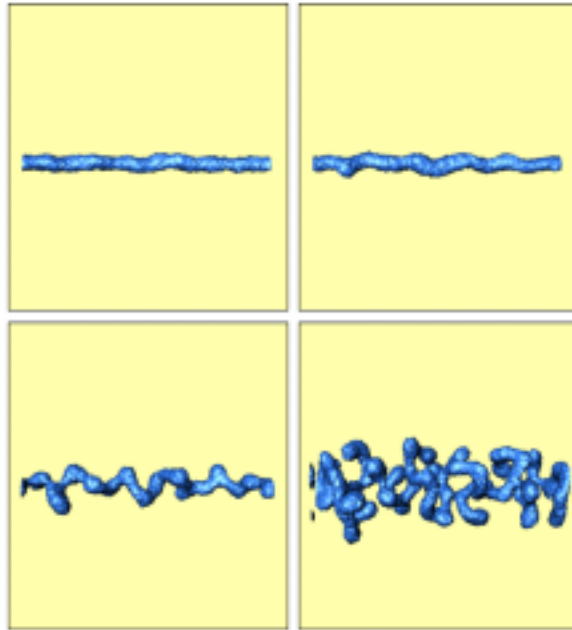


Figure 3: Evolution of a three-dimensional labyrinthine pattern. Reaction rate constants are $\bar{k}_1 = 4.2$, $\bar{k}_1^* = 4.2$, $\bar{k}_2 = 0.4$, $\bar{k}_3 = 0.1$ and $D_v/D_u = 4$. Panels (top to bottom and left to right) correspond to 10, 20, 40, 80 ($\times 1,000$) automation steps. When the simulation is carried out for larger times the three-dimensional labyrinthine patterns fills the entire domain.

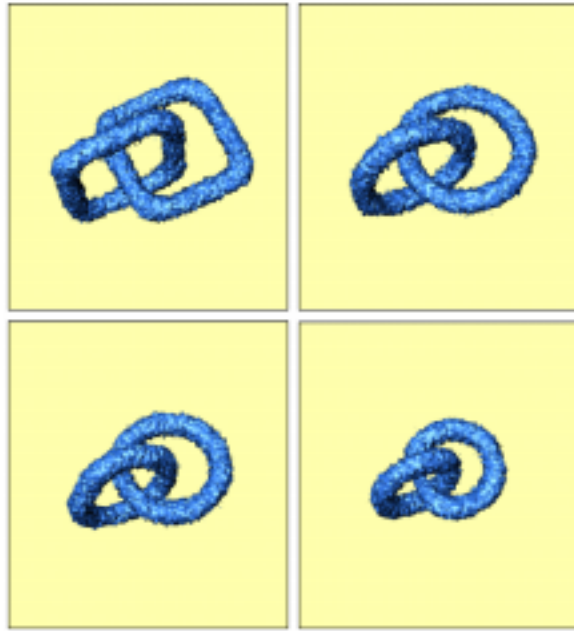


Figure 4: A stable Hopf link. Reaction rate constants are $\bar{k}_1 = 4.31$, $\bar{k}_1^* = 3.8$, $\bar{k}_2 = 0.4$, $\bar{k}_3 = 0.06$ and $D_v/D_u = 4$. Panels (top to bottom and left to right) correspond to 10, 80, 320, 1280 ($\times 1,000$) automation steps.

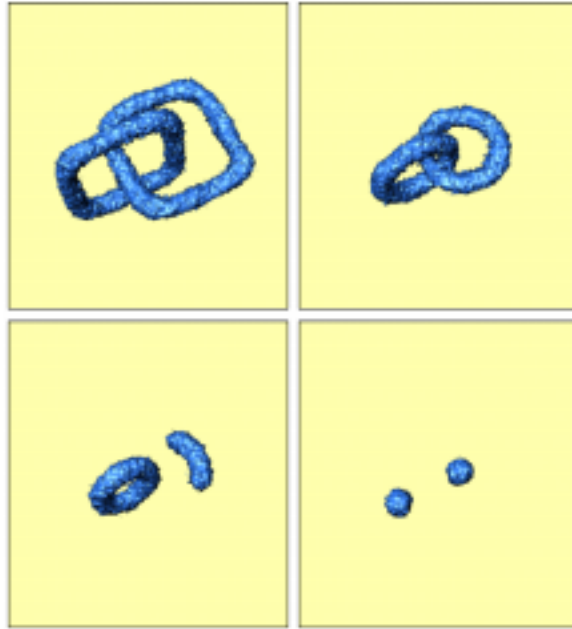


Figure 5: Evolution of a link in media with weak front repulsion. Reaction rate constants are $\bar{k}_1 = 4.1$, $\bar{k}_1^* = 3.8$, $\bar{k}_2 = 0.4$, $\bar{k}_3 = 0.2$ and $D_v/D_u = 4$. Panels (top to bottom and left to right) correspond to 10, 160, 320, 640 ($\times 1,000$) automation steps.

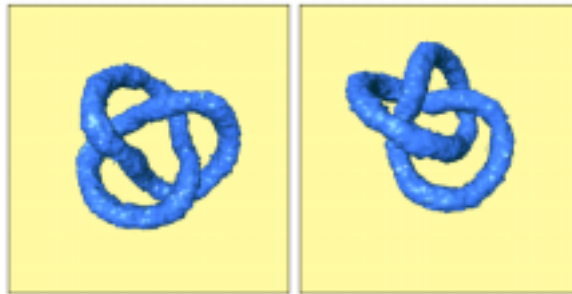


Figure 6: A trefoil knot. Reaction rate constants are $\bar{k}_1 = 4.1$, $\bar{k}_1^* = 3.8$, $\bar{k}_2 = 0.2$, $\bar{k}_3 = 0.07$ and $D_v/D_u = 4$. This simulation was performed with slightly different lattice-gas rules. The existence of stable knots is independent of such rule changes.

from equilibrium chemical systems. While some aspects of the statistical mechanics of this complex system have been investigated [8], a full treatment of the microscopic dynamics remains a challenging task. In addition, the ability to efficiently simulate such dynamics on the CAM-8 machine has allowed us to study complex three-dimensional pattern formation processes.

References

- [1] R. FitzHugh, *Biophys. J.* **1**, 445 (1961); J. Nagumo, S. Arimoto and Y. Yoshikawa, *Proc. IRE* **50**, 2061 (1962).
- [2] T. Ohta, A. Ito and A. Tetsuka, *Phys. Rev. A* **42**, 3225 (1990); T. Ohta, R. Mimura and M. Kobayashi, *Physica D* **34**, 115 (1989).
- [3] A. Hagberg and E. Meron, *Phys. Rev. Lett.* **72**, 2494 (1994); C. Elphik, A. Hagberg and E. Meron, *Phys. Rev. E* **51**, 3052 (1995).
- [4] D. M. Petrich and R. E. Goldstein, *Phys. Rev. Lett.* **72**, 1120 (1994); R. E. Goldstein, D. J. Muraki and D. M. Petrich, *Phys. Rev. E* **53**, 3933.
- [5] K. J. Lee, W. D. McCormack, Q. Ouyang and H. L. Swinney, *Science* **261**, 192 (1993); K. J. Lee and H. L. Swinney, *Phys. Rev. E* **51**, 1899 (1995); K. J. Lee, W. D. McCormack, J. Pearson and H. L. Swinney, *Nature* **214**, 215 (1994).
- [6] J. P. Boon, D. Dab, R. Kapral and A. Lawniczak, *Phys. Repts.* **273**, 55 (1996).
- [7] A. Malevanets and R. Kapral, *Phys. Rev. Lett.* **77**, 767 (1996).
- [8] A. Malevanets and R. Kapral, *A Microscopic Model for FitzHugh-Nagumo Kinetics*, *Phys. Rev. E*, submitted.
- [9] U. Frisch, D. d'Humieres, B. Hasslacher, P. Lallemand, Y. Pomeau and J.P. Rivet, *Complex Systems* **1**, 649 (1987).
- [10] N. Margolus, in *Pattern Formation and Lattice-Gas Automata*, edited by R. Kapral and A. Lawniczak (Fields Institute Communications, AMS, Providence, 1996), p.165.

- [11] P. Coulet, J. Lega, B. Houchmanzadeh, and J. Lajzerowich, *Phys. Rev. L* **65**, 1352 (1990).
- [12] P. C. Hohenberg and B. I. Halperin, *Rev. Mod. Phys.* **92**, 435 (1977).
- [13] D. Haim, G. Li, Q. Ouyang, W. D. McCormick, H. L. Swinney, A. Hagberg and E. Meron, *Phys. Rev. Lett.* **77**, 190 (1996).